



## Modeling hydrography and marine sedimentation in the Cariaco Basin since the Last Glacial Maximum

G. F. Lane-Serff<sup>1</sup> and R. B. Pearce<sup>2</sup>

Received 7 August 2008; revised 12 January 2009; accepted 3 February 2009; published 10 April 2009.

[1] The Cariaco Basin has shallow connections with the Caribbean Sea, and these are further reduced at times of lower sea level, such as at the Last Glacial Maximum (LGM). A numerical model was developed to describe the oceanography and biogenic sedimentation in the Cariaco Basin and nearby Caribbean. The model is run with different sea levels in order to simulate the changing oceanography and the development of deep water anoxia in the Cariaco Basin since the LGM. In the main sequence of numerical experiments, the surface forcing is kept fixed at present-day values while the sea level is changed in order to separate the effects of sea level from the effects of climate. As the sea level rises, the main sedimentation zone moves first to the shallow broad northern sill and NE part of the Cariaco Basin and then, once sea level reaches approximately 60 m below present, moves south to the northern coast of mainland Venezuela. The model shows that there would be an overall increase in sedimentation in the basin as the sea level rises, even if there was no change in the surface forcing. However, the model also shows that sedimentation at particular points in the basin exhibits more complicated behavior, which needs to be taken into account when interpreting individual records. Preliminary numerical experiments examine the effects of changing surface forcing while keeping the sea level at LGM values, and the applicability of a mathematical hydraulic control model in this case is also considered.

**Citation:** Lane-Serff, G. F., and R. B. Pearce (2009), Modeling hydrography and marine sedimentation in the Cariaco Basin since the Last Glacial Maximum, *J. Geophys. Res.*, 114, C04003, doi:10.1029/2008JC005076.

### 1. Introduction

[2] The Cariaco Basin lies to the north of Venezuela and covers an area approximately 200 km east-west by 100 km north-south (Figure 1). It consists of two subbasins, both reaching a depth of 1400 m, separated by a central saddle of depth 1000 m. The Basin is surrounded by islands and shallow banks, mostly with a depth of less than 100 m, the only deeper connections to the rest of the Caribbean being a narrow channel to the north-west (between the Island of Tortuga and the mainland) with a maximum depth of 146 m and a broader, shallower channel of depth 120 m to the north (between Tortuga and Margarita). With this topography the Basin is currently anoxic below about 300 m [Richards, 1975], promoting good preservation of laminated marine sediments. The prevailing trade winds create strong upwelling conditions and high primary productivity, which is reflected in the relatively high biogenic sedimentation rates and laminated sedimentary record. However, the high total sedimentation rates in the Cariaco Basin are primarily a

result of the significant input of terrigenous material from local rivers (the main ones being the Rio Tuy and Rio Unare), peaking during and following the rainy season (June to November) [Peterson and Haug, 2006].

[3] The sedimentary record in the Cariaco Basin has been widely studied using numerous piston cores and more recently drilled cores at ODP Site 1002 [e.g., Peterson *et al.*, 1991; Hughen *et al.*, 1996; Lin *et al.*, 1997; Peterson *et al.*, 2000a; Lea *et al.*, 2003]. The onset of the present anoxic conditions within the Basin and the preservation of laminated sediments began at approximately 14,700 calendar years before present (ka B.P.) [Peterson *et al.*, 1991; Hughen *et al.*, 1996]. In Figure 2 the main time interval of interest (15–11 ka B.P.) is marked, along with the preservation state of laminated sediments at ODP Site 1002. The rise in sea level against time has also been plotted in Figure 2 [from Fairbanks, 1989]. The changes in sea level have an impact on the sill connections between the Cariaco Basin and the Caribbean Sea. This in turn affects oceanographic circulation and nutrient supply to the Basin, so that changes in sea level give rise to changes in the sedimentary record, which is independent of climate forcing [Peterson *et al.*, 1991; Lin *et al.*, 1997; Haug *et al.*, 1998]. For example, there is a marked correlation between sea level and total organic carbon (TOC) indicating a sea level control on export productivity within the basin [Haug *et al.*, 1998].

<sup>1</sup>School of Mechanical, Aerospace and Civil Engineering, University of Manchester, Manchester, UK.

<sup>2</sup>School of Ocean and Earth Science, University of Southampton, National Oceanography Centre Southampton, Southampton, UK.

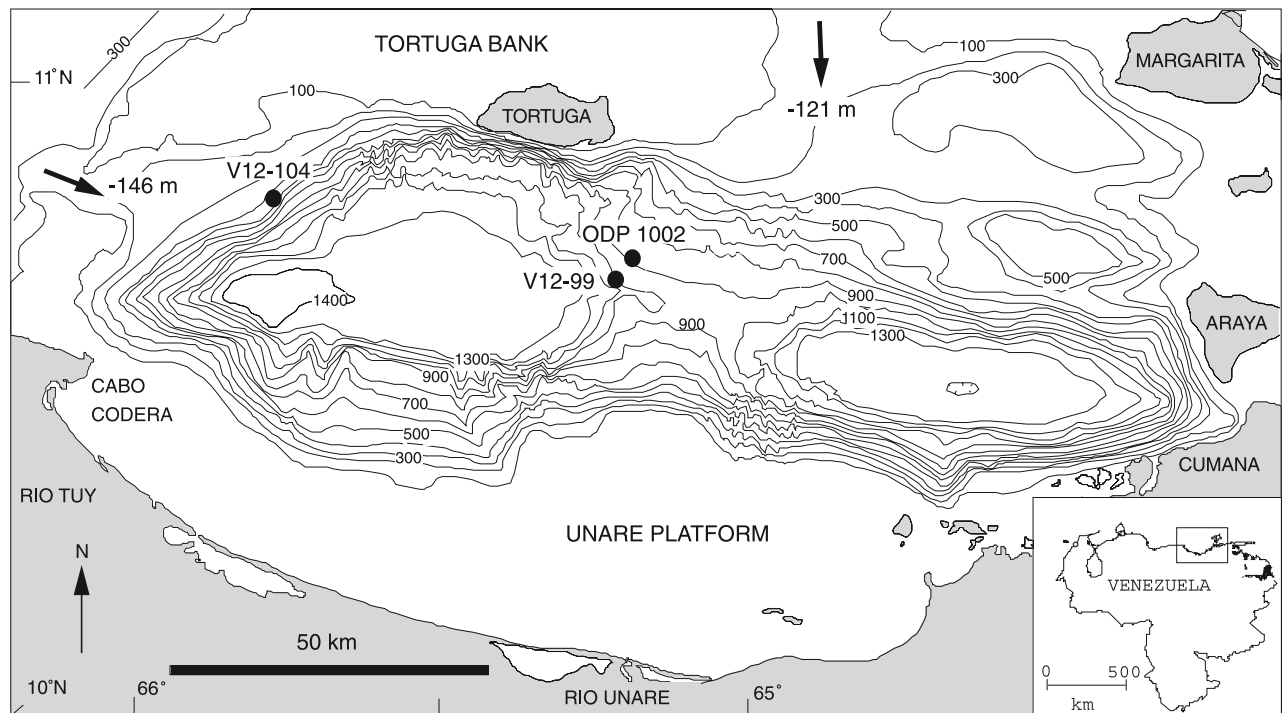


**Figure 1.** Modern bathymetric map of the Cariaco Basin showing the location of the cores referred to in this study. Arrows indicate the principal sills through which exchange with the Caribbean Sea occurred during the Last Glacial Maximum to the beginning of the Holocene. The sill depths in the modern basin are also included. Inset shows the location of the Cariaco Basin on the north coast of Venezuela.

[4] During the last glacial it has been suggested that a major locus of upwelling was seaward of the emergent Tortuga Bank [Peterson *et al.*, 1991], but that upwelling was still physically active in the Cariaco Basin, and comparable to Holocene upwelling rates [Lin *et al.*, 1997]. It has been proposed that nutrients entering the Basin were sourced from the near-surface nutrient-depleted waters in the open Caribbean Sea, leading to only low productivity plankton assemblages, with reduced oxygen demand, and as a consequence the deeper Basin waters remained oxygenated [Peterson *et al.*, 1991; Lin *et al.*, 1997]. During the transition from the last glacial there is evidence for enhanced Ekman-driven upwelling, a corresponding rise in primary and export production, an increased rate of sea level rise and a likely influx of nutrient-rich subthermocline waters [Lin *et al.*, 1997; Haug *et al.*, 1998; Peterson *et al.*, 2000a]. Following on from these changes, the rate of oxygen replenishment by circulation in the deep basin was insufficient to prevent the rapid onset of anoxia, a feature that has persisted to the present day. Other likely sources of nutrients into the Basin are from local rivers [Peterson *et al.*, 2000b], and the onset of anoxia at 14.7 ka B.P. probably corresponds to an abrupt increase in riverine discharge as noted from the transition from dry- to wet-type vegetation [Hughen *et al.*, 2004]. Although biogenic sedimentation has a significant influence on the sedimentary record in the Cariaco Basin, the region is still a terrigenous dominated system, with such sediments comprising 35–90 weight% of total sedimentation [Peterson *et al.*, 2000a].

[5] In this paper a sophisticated numerical model is described, which is able to predict biologically mediated

sedimentation from primary production. The model does not attempt to simulate the entire system, for which a very complex model would be required, but instead focuses on the changes in oceanographic circulation and flux of nutrients from the Caribbean Sea in response to some basic changes in surface forcing and sea level. This is the first study to use a detailed numerical ocean model to investigate the paleoceanography of the Cariaco Basin. The model

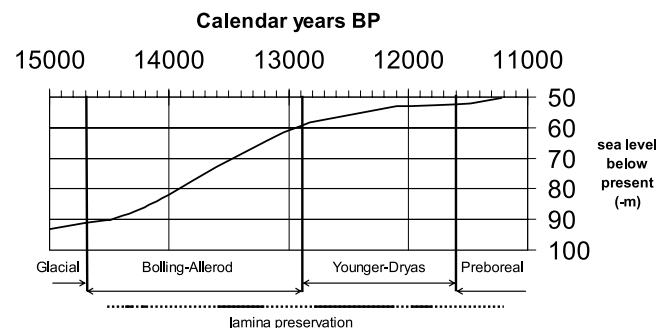


**Figure 2.** Sea level curve [after Fairbanks, 1989] for the time interval 15–11 ka B.P. together with the occurrence of laminated sediments examined from ODP Site 1002. The solid line denotes very well laminated sediments showing little or no evidence of bioturbation from thin-section analyses, and the dotted lines represent intermediately laminated sediments, i.e., those showing some evidence of bioturbation and disturbance. Sediment chemistry indicates that anoxic conditions occur throughout the postglacial period [Dean *et al.*, 1999].

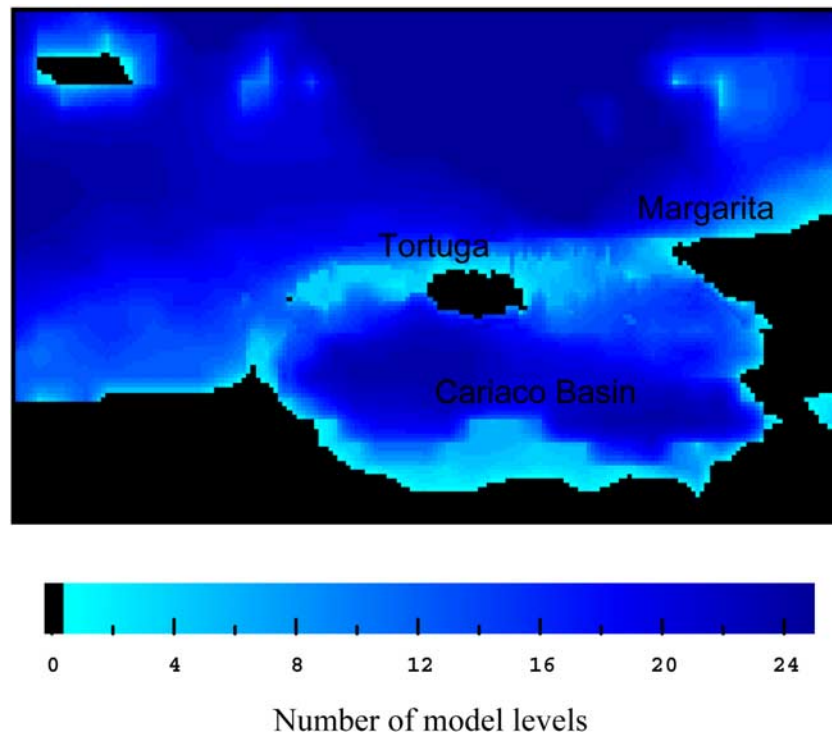


**Figure 3.** Model topography for sea level 50 m below present: The Cariaco Basin occupies the southeastern part of the model domain. Black marks land, while the paler shades of blue mark shallower water (fewer model depth levels). The Island of Tortuga is similar to its present-day shape, but the Island of Margarita is still joined to the mainland (eastern side of the domain).

allows us to address more directly and quantitatively some of the results inferred from the paleoceanographic record (such as those given above) and gives a means for investigating spatial variability for given time slices.

[6] First the model is used to make some preliminary investigations of the likely effect of different surface forcing on biogenic sedimentation at a time of low sea level (120 m below present) corresponding to the Last Glacial Maximum (LGM) at approximately 21 ka B.P. There is also a brief consideration of simpler sill-basin models applied to this case. The main part of the investigation is to use the numerical model to examine how changes in sea level affect sedimentation within the Cariaco Basin while keeping the surface forcing fixed. The sea levels studied range from 120 m below present to 50 m below present, equivalent to the period from the LGM to 11 ka B.P. After this time the shallower connections to the east become open, and this would require a numerical model covering a larger area to adequately define the region surrounding the Cariaco Basin with more complicated boundary conditions.

[7] In the next section the details of the numerical model are described, followed by a section describing the numerical experiments conducted. Next the model results are described and discussed. This includes a comparison between a simple sill-basin model and the LGM model results with a range of climate conditions. The main results from the model are also described, showing how primary production increases within the Cariaco Basin as sea level increases. It is also shown how the behavior at individual locations within the Basin (such as the ODP site) may be more complicated than the broad, overall picture. In the

final section the implications of the results of the numerical model for the interpretation of the sedimentary record are discussed and future areas of research are described.

## 2. Numerical Model

[8] The model covers the region between  $67^{\circ}\text{W}$  to  $64^{\circ}\text{W}$  and  $10^{\circ}\text{N}$  to  $12^{\circ}\text{N}$ . The model topography, for sea level 50 m below present, is shown in Figure 3. The topography was derived by linear interpolation from the ETOPO5 data set ( $5'$  resolution [NOAA, 1988]) onto the model grid, which has a resolution of  $1'$  (approximately 2 km). The topography was adjusted by hand with reference to charts, especially at the shallow straits. Higher-resolution data sets [e.g., Smith and Sandwell, 1994, 1997] were considered part way through the modeling, but these were found to be particularly poor near coasts and shallow regions, and would have required similar adjustments.

[9] In the vertical the domain is divided into boxes whose thickness increases with depth. The surface layer (level 1) is 4 m thick and each successive layer is a factor  $2^{1/3}$  larger than the previous one, with the lowest box (level 25) 256 m thick. The higher resolution near the surface allows accurate representation of the surface layers, while the deep water is largely stagnant and thicker layers are adequate for resolving the deposition processes. The main purpose of the part of the model outside the Cariaco Basin is to provide the correct conditions in the neighborhood of the shallow sills, rather than to provide an accurate simulation of the flow throughout the modeled region. In this paper the sea level is always at least 50 m below its present level.

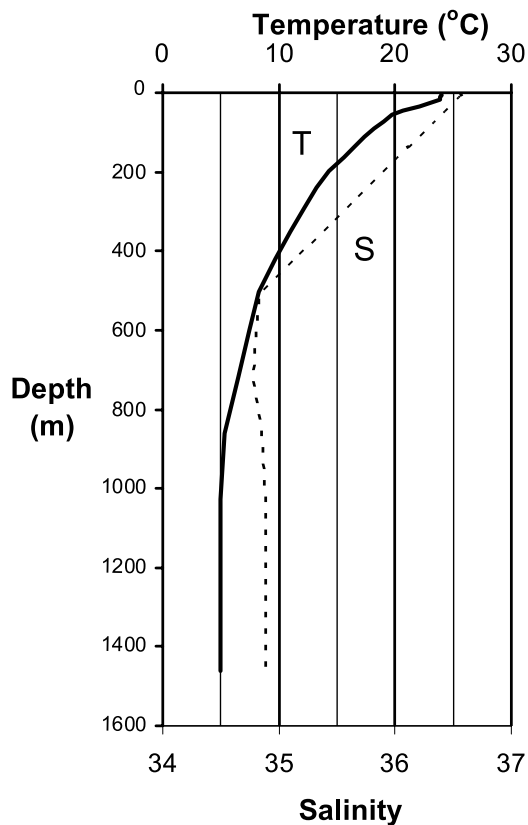


**Figure 4.** The temperature and salinity profiles used at the lateral boundaries of the model.

[10] The numerical model itself is a modified version of the OCCAM model [Webb, 1993, 1998], which in turn follows the format of the GFDL Modular Ocean Model [Pacanowski *et al.*, 1990]. The model has an explicit free surface, and one of the modifications made for this study was to implement a surface freshwater scheme. Thus the free surface rises and falls in response to precipitation and evaporation, and the salinity is adjusted to conserve salt. The horizontal eddy viscosity and eddy diffusivity were set to the smallest (fixed) values that did not give numerical instability: These were  $4.3 \times 10^6 \text{ cm}^2 \text{ s}^{-1}$  and  $8.7 \times 10^6 \text{ cm}^2 \text{ s}^{-1}$  respectively. The model time steps were set to be as large as possible while maintaining stability, with final values of 6 seconds for the barotropic steps (to cope with the free surface) and 180 seconds for the baroclinic and advective steps.

[11] The model was stable with a uniform vertical eddy viscosity and diffusivity of  $1 \text{ cm}^2 \text{ s}^{-1}$  (a commonly suggested value for the deep ocean), but this allowed an unrealistic shear between the wind-driven upper layer and the layers below (there is no surface mixed layer parameterization in the model). Therefore a Richardson number (Ri) dependent vertical mixing scheme was developed, with the vertical eddy viscosity and diffusivity both varying from 1 to  $50 \text{ cm}^2 \text{ s}^{-1}$  as a linear function of Ri for values of Ri between 0.8 to 0. The convective adjustment scheme was also modified so that where dense water overlies less dense water the water properties are swapped (in so far as the different box sizes allows) rather than completely mixed (as in the original model). As might be expected, it was only

when deep convection occurred (the “very dry” run described in the next section) that the different convection schemes showed any marked effect on the results (and even then only a fraction of a degree change in sea surface temperature, for example).

[12] The boundaries of the domain are treated as solid walls. A lateral boundary condition scheme was introduced, relaxing the tracers to “Caribbean profiles” in the outer ten grid boxes at the west, north and east edges of the domain outside the Cariaco Basin. The Caribbean T-S profiles were obtained from Richards and Vaccaro [1956], with a simplified structure in the top 50 m (Figure 4). The relaxation is more rapid toward the edge of the domain, with a relaxation timescale of one day in the outermost grid boxes and the relaxation timescale increasing with distance from the boundary to a timescale of ten days for grid boxes ten points from the boundary. The free surface height is relaxed to zero in the same zone. This effectively removes any large-scale flow that may be present in the Caribbean but, as we show below, the main upwelling circulation in the southern part of the domain is captured.

[13] In addition to temperature and salinity, three further tracers were added (nutrient, oxygen and detritus) that form the components of a simple biochemical model. This model is very similar to that given by Stratford *et al.* [2000]. Here nutrient is interpreted as nitrate, since this is generally regarded as the main limiting nutrient in the Cariaco Basin. However, since there is evidence of nitrogen fixation in the Cariaco Basin [Haug *et al.*, 1998] and given that the only source for nutrient in the model is outside the Cariaco Basin, it may be better to regard the nutrient as the equivalent amount of nitrate made available for production by the advection of phosphate from the Caribbean. The purpose of our model is not to recreate the complete biogeochemical system, but to isolate and investigate the effect of the extra nutrient advected into the Cariaco Basin as a result of sea level change.

[14] Nutrient, N, is converted into detritus, D, at a rate  $\lambda$  that depends upon the available sunlight and nutrient concentration, with a maximum value,  $\lambda_0$ , such that  $1/\lambda_0 = 3$  weeks (i.e., the timescale for converting nutrient to detritus is three weeks or longer). The average daily sunlight at the surface varies through the year and is given by a simple model based on latitude and time of year, with no allowance for shading by clouds or biology (Figure 5), represented by the function  $s(t) \leq 1$ . Though some cloud shading could have been included, it would have introduced an extra complicating factor and relatively small variations

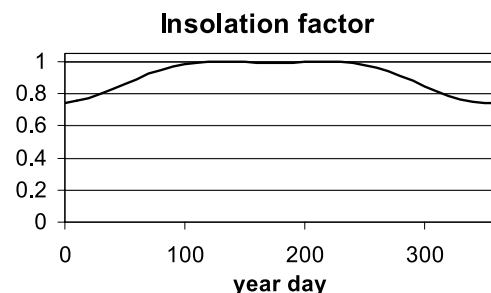


**Figure 5.** Insolation factor  $s(t)$  showing the variation in the relative amount of total sunlight throughout the year.

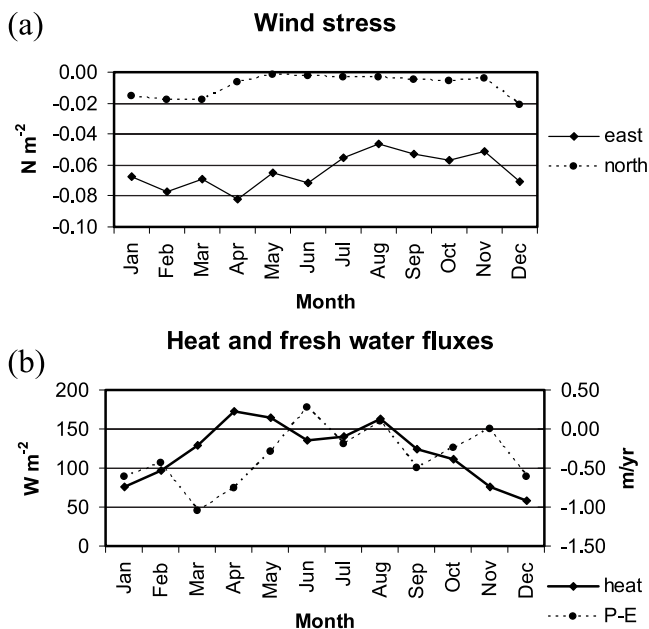


**Figure 6.** Surface forcings (based on present-day conditions from *Josey et al.* [1999]) used to drive the model: (a) wind stress (note predominantly SW direction) and (b) heat and net freshwater flux.

in sunlight were not found to have a large effect on the overall results in any case (once the nutrients are near the surface, variations in sunlight only have a marginal effect on the time taken to convert the nutrient to detritus and little effect on the total sediment load produced). The sunlight decreases exponentially with depth, with a fixed  $e$ -folding length scale of 20 m. Detritus is remineralized back into nutrient at a rate  $r$  that depends on the oxygen concentration, consuming oxygen in the process. A fixed  $O_2:N$  Redfield ratio appropriate to remineralization is assumed, with the value  $R = 10.6$  taken from *Anderson and Sarmiento* [1994]. The equations for the biochemical processing are

$$\begin{aligned}\frac{\partial D}{\partial t} &= \lambda N - rD \\ \frac{\partial N}{\partial t} &= -\lambda N + rD \\ \frac{\partial O_2}{\partial t} &= -RrD\end{aligned}$$

$$\lambda = \lambda_0 e^{-zk} s(t)$$

where the reaction rate  $r = 0.44 \text{ day}^{-1}$  if the oxygen concentration is greater than  $0.06 \text{ mol m}^{-3}$  and varies linearly down to  $r = 0.15 \text{ day}^{-1}$  as the oxygen concentration decreases to zero (as in the work of *Stratford et al.* [2000]). The oxygen levels in the surface layer of the ocean are assumed to be at the equilibrium value, since the timescales for gas transfer are relatively fast. The actual equilibrium value depends on temperature and salinity, but here we take a fixed value of  $0.2 \text{ mol m}^{-3}$  for simplicity. In practice in most runs the oxygen level was well above  $0.06 \text{ mol m}^{-3}$  everywhere, because most runs started from a well-

oxygenated state (concentration equal to  $0.2 \text{ mol m}^{-3}$  everywhere) and it would take many years for the oxygen in the deep water to be removed. However, the model was used to indicate the rate at which oxygen is consumed and thus the timescales needed to develop anoxia.

[15] The nutrient, detritus and oxygen are advected in the same way as temperature and salinity, but in addition detritus is advected vertically with a specified fall velocity of 200 m per day. This vertical advection is dealt with using a separate simple first-order upwind scheme as attempts to incorporate it into the main advection scheme led to severe numerical instabilities. Any detritus reaching the sea floor is collected as “sediment” and takes no further part in the biochemical model. The annual layers of terrigenous sediment, mostly washed into the Basin from surrounding rivers, form an important part of the observed laminated sediment but have not been incorporated into the present model.

### 3. Numerical Experiments

[16] Initially the nutrient concentration is set to  $0.07 \text{ mol m}^{-3}$  in water outside the Cariaco Basin below 100 m, based on the nitrate value found in the Subtropical Underwater by *Walsh et al.* [1999]. Subsequently, at the domain boundaries nutrient is relaxed to its original value in the same way as temperature and salinity. This means that the only source for nutrient in the Cariaco Basin in this model is from the deep water that was originally outside the Basin, and we are limiting our attention to this source here. Thus we are ignoring nutrient that is supplied by the local rivers and also any nutrient fixed in the Cariaco Basin.

[17] The main model runs use a fixed annual cycle of surface forcing but consider different sea levels. The surface fluxes of heat, freshwater and wind stress used in the main runs (Figure 6) are given by linear interpolation of monthly mean values based on the Southampton Oceanography Centre (SOC) climatology [*Josey et al.*, 1999]. Given the relatively small area covered by the Cariaco Basin compared with the SOC climatology resolution, we use spatially uniform surface fields. In each experiment the model was run for a model time of at least ten years. This is long enough to establish the main features of the ocean circulation but slow processes (such as developing anoxia in the deep waters of the Cariaco Basin) happen on much longer timescales (not attempted here). The timescale for the development of anoxia is estimated by extrapolation of the runs (see below). Note that there is no run allowing direct comparison with present-day conditions and topography: This would require a larger model domain and more sophisticated boundary conditions to allow for the effect of coastal flows coming into the Cariaco Basin through the shallow passages to the east (not open during the times of the paleoexperiments run here).

#### 3.1. Climate Change at LGM Sea Levels

[18] In the first series of experiments consisting of three runs (“LGM series”), the sea level was fixed at 120 m below its present value, corresponding approximately to LGM conditions. At this time there was only a single channel connecting the Cariaco Basin to the rest of the Caribbean, situated in the northwest of the Basin between

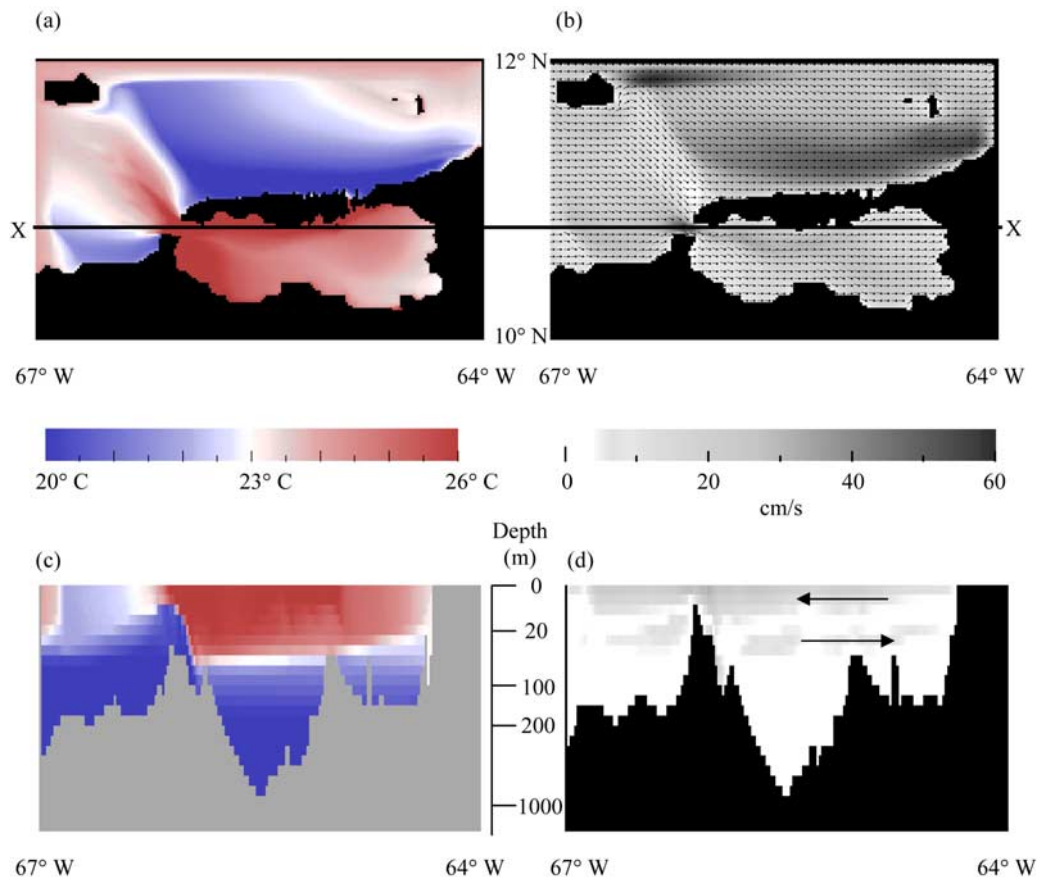


**Figure 7.** Model results for sea level 120 m below present and with present-day fluxes (from the end of a ten-year run): (a) sea surface temperature, (b) surface velocity (with direction indicated by the lines starting at the dots and speed shown by the gray scale), (c) temperature on a W-E section through the Cariaco Basin, and (d) flow speed on a similar W-E section (arrows indicate main flow direction in the Cariaco Basin). Note the nonlinear depth scale and also that the velocity and temperature are on staggered grids so that the effective topography is not identical. The position of the W-E sections are marked X-X in Figures 7a and 7b.

Tortuga and the mainland. The channel would have been approximately 15 km wide and 30 m deep. It has been suggested that the Intertropical Convergence Zone (ITCZ) was on average further south during the LGM [e.g., Chiang *et al.*, 2003] and so in the second run this was simulated by using surface fluxes derived from present-day fluxes but from 2° further north. Finally, a third, “very dry” climate was imposed, based on the one just described but with higher evaporative fluxes: approximately  $50 \text{ W m}^{-2}$  higher in terms of the evaporative cooling flux, with a corresponding increase in the (evaporative) freshwater flux (equivalent to an extra evaporation of approximately 0.6 m/year). This was primarily to observe how the flow behaved under forcing strong enough to produce deep convection, rather than to simulate any particular climate scenario.

### 3.2. Changing Sea Level

[19] The model was then run for sea levels 120 m, 100 m, 80 m, 70 m, 60 m and 50 m below present. These sea levels correspond approximately to the times 21 ka B.P., 16 ka B.P., 14 ka B.P., 13.5 ka B.P., 13 ka B.P. and 11 ka B.P., respectively. Of course, it is also appropriate for earlier (pre-

LGM) time intervals with this range of sea levels provided the Cariaco Basin topography is close to the present-day configuration. The sea level is not altered during the course of a run, so that the results are not dependent on the sea level model used: The results represent short time slices at fixed sea level, not data extracted at intervals from a very long continuous run. The surface forcing is equivalent to present-day conditions throughout. This is clearly not accurate for the end of the glacial period or, for example, during the Younger Dryas, but it allows us to separate the effects of sea level change from the effects of climate.

## 4. Results and Discussion

### 4.1. Response to Climate Change at LGM Sea Levels

[20] Output from the model after ten model years with LGM sea level but present-day surface fluxes is shown in Figure 7. Overall the surface fluxes make the waters in the Basin less dense and a two-layer exchange flow is set up through the channel, with denser water entering the Basin at depth and warmer, lighter water leaving the Basin at the surface. The dense water entering the Basin does not

**Table 1.** Approximate Time to Develop Anoxia From a Fully Oxygenated State in the Deep Waters of the Cariaco Basin<sup>a</sup>

Sea Level (Below Present; m)	Approximate Time to Develop Anoxia (Years)	
	West Subbasin	East Subbasin
120	550	375
100	300	250
80	225	150
70	175	100
60	900	200
50	400	250

<sup>a</sup>The estimate is based on the reduction in oxygen at a depth of approximately 1000 m in the center of the two subbasins during the last 4 to 6 years of each model run.

penetrate to any great depth inside the Basin, so that the main circulation is confined to the top 100 m or so of the water column. The dense water flows from west to east across the Basin, upwelling mainly at the eastern side of the Basin before returning to the west at the surface. The biological activity and sedimentation is concentrated in this upwelling region, where the nutrient is brought into the surface waters (which have sufficient sunlight for significant nutrient utilization). As the surface water flows eastward it is warmed, giving a maximum east-west difference in sea surface temperature (SST) of approximately 3.5°C between the SE corner of the Basin and the NW strait. The difference between SST and the temperature at 100 m depth is approximately 4°C in the eastern subbasin, rising to 5°C in the western subbasin. The warm waters leaving the Cariaco Basin flow north west, with a sharp front between these waters and the relatively cool waters upwelling to the north of Tortuga.

[21] Below the main circulation the water is essentially stagnant and the remineralization of falling detritus slowly removes oxygen from the deep water. However, the amount

of nutrient brought into the Basin is relatively small so that the rate at which oxygen is consumed suggests it would take of the order of 375 years to develop anoxia in the deep water (>1000 m) in the eastern subbasin and 550 years in the western subbasin (starting from a fully oxygenated state), see Table 1.

[22] With the surface fluxes based on a more southerly ITCZ position, the annual buoyancy flux still produces less dense water, so that the main features of the circulation (and biogeochemical fluxes and processes) are essentially the same as before. However, for the artificially very dry climate, dense waters were produced during part of the year, leading to deep convection. The deep convection would occur first in the eastern subbasin beginning in May/June each year, filling that subbasin with dense oxygenated water which would flow over the central saddle and into the western subbasin around August/September (Figure 8).

[23] In summary, the flow in the Cariaco Basin is likely to be estuarine-like in character with less dense water flowing out of the Basin at the surface and denser water entering the Basin underneath. The incoming water does not penetrate to great depth, so the deep water is essentially stagnant and thus the development of anoxia is likely. It would require an extremely dry climate to produce deep convection within the Cariaco Basin, with an “antiestuarine” type circulation. It is possible that replenishment of oxygen in the deep water comes from occasional flushing events when water denser than the Cariaco deep water enters the Basin from outside.

[24] Thus, at sea levels characteristic of the LGM, both the present-day climate and a more realistic LGM climate give similar patterns of circulation (and sediment distribution) within the Cariaco Basin. Changes in forcing are thus more likely to affect the strength of the circulation, and the amount of primary production and sedimentation, while the circulation pattern remains unaltered. However, the circulation pattern will be significantly affected by the changes in

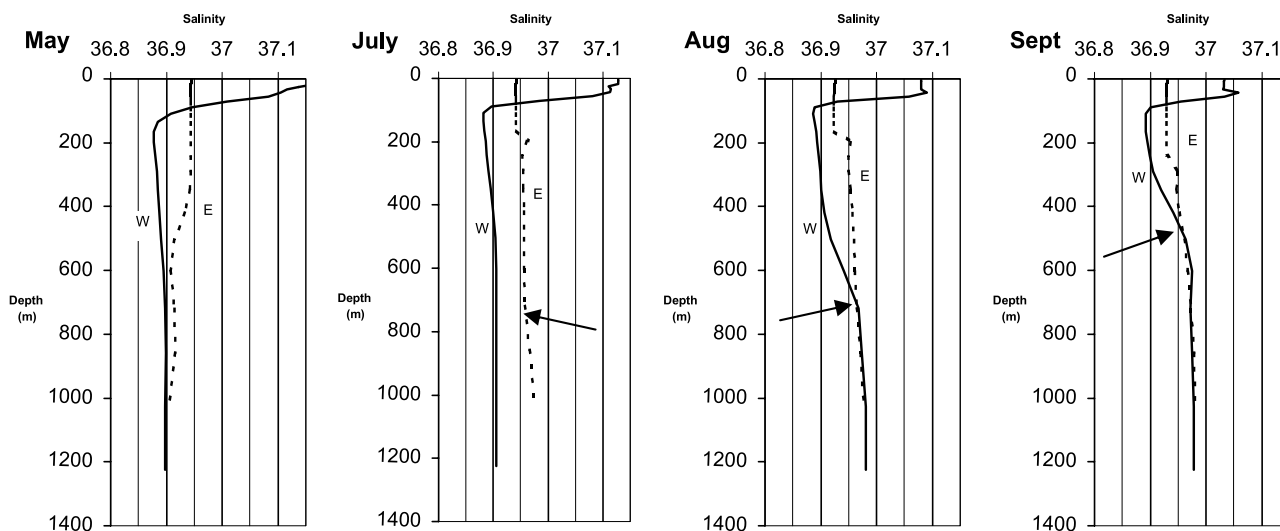


**Figure 8.** Model results for salinity profiles from the west and east subbasins of the Cariaco with “very dry” forcing and sea level 120 m below present. The west subbasin is marked with solid lines, and the east is marked by dotted lines. Note the saline waters filling the east subbasin between May and July and then filling up the west subbasin during August and September (arrowed).

**Table 2.** Density Contrast Found in the Numerical Model and in the Sill Model Between the Waters Inside the Cariaco Basin and Those Outside at Sill Depth Under Various Forcing Regimes

	Mean Total Buoyancy Flux ( $\times 10^2 \text{ m}^4 \text{ s}^{-3}$ )	Density Contrast ( $\text{kg m}^{-3}$ )	
		Numerical Model	Sill Equation
Present-day fluxes	-13.9	-1.63	-1.78
“LGM” fluxes	-3.7	-0.42	-0.66
“Very dry” fluxes	+3.1	1.29	0.66

topography considered later. Next we consider how the LGM circulation can be modeled using a simple hydraulic model.

#### 4.2. Comparison of LGM Results With a Simple Hydraulic Model

[25] For a semienclosed sea with a single connection to the rest of the ocean it is possible to use a hydraulic model of the exchange flow over the sill to relate the density contrast between the inflowing and outflowing waters to the imposed buoyancy flux. This is based on the idea that, in a steady flow, the buoyancy flux at the sill must be the same as the total buoyancy flux for the Basin as a whole (e.g., as applied to the Mediterranean by *Bryden and Kinder* [1991] and to the Black Sea by *Lane-Serff et al.* [1997]). The details depend on the precise shape of the channel [*Dalziel*, 1992] but a reasonable approximation can be found by assuming the interface between the two water masses is at half the channel depth. For a channel of depth  $H$  and width  $W$  (in m), the relative density contrast  $\Delta\rho/\rho$  is approximately related to the buoyancy flux  $B$  (in  $\text{m}^4 \text{ s}^{-3}$ ) by

$$\frac{\Delta\rho}{\rho} = \frac{1}{gH} \left( \frac{4B}{W} \right)^{2/3},$$

where  $g$  is the gravitational acceleration.

[26] The density contrast predicted from the annual mean fluxes for the three different imposed surface fluxes using this equation is compared with the density contrast observed in the corresponding runs of the numerical model (looking at the inflowing and outflowing layers just inside and outside the Basin) in Table 2. Overall the response to changing buoyancy forcing in the numerical model is similar to that predicted using the simple sill model. However, the wind-driven circulation (not included in the sill model) is clearly having an effect. The wind stress tends to increase the westward flow in the upper layer out of the Cariaco Basin. When the buoyancy forcing also produces a westward flowing upper layer the strength of the circulation is stronger than if it were just driven by the density contrast, so a slightly weaker density contrast is needed to achieve the same buoyancy flux. Conversely, when the buoyancy forcing is producing a circulation in the opposite sense, as it does for the “very dry” case, then the wind forcing is opposing the buoyancy forcing. Thus a larger density difference is required to overcome the wind forcing and produce the required buoyancy flux. Furthermore, the circulation in the channel in the numerical model is more complicated in this last case, with the wind stress forcing

some surface water out of the Basin and so there is not a simple two-layer exchange flow.

#### 4.3. Response to Sea Level Change

[27] Returning to the numerical model, as the sea level rises, the link to the Caribbean to the north (between Tortuga and Margarita) begins to open. A similar flow is observed in both the northwestern and northern straits, with dense water flowing into the Basin at depth and surface water flowing north and west out of the Basin. The surface outflow is generally stronger to the west of Tortuga. For sea level between 120 m and 80 m below present, the upwelling of cooler waters is strongest in the east of the Basin. The peak flow speeds remain similar, but the larger openings now allow a greater overall flow so that the surface waters do not have time to be warmed so much as they flow from east to west. As a result the temperature difference between the surface waters and the waters at 100 m depth reduces to approximately  $2^\circ\text{C}$  in the eastern subbasin and  $2.5^\circ\text{C}$  in the western subbasin. As the sea level rises to 50 m below present, the region of upwelling extends to the southern side of the Basin, over the now submerged Unare Platform.

[28] For all the sea level change experiments, the flow in the Basin is confined to the upper 200 m or so of the water column, with the deep waters remaining stagnant. Oxygen is steadily removed from the deep water by the remineralization of detritus falling from the upper productive areas. All of the runs were started from a fully oxygenated state and the timescale for developing anoxia in the deep water can be estimated from the rate at which the oxygen concentration in the deep water decreases (Table 1). It is emphasized that these results are a best estimate of (sometimes) very long timescales based on ten to fifteen year simulations, so the results should be treated with some caution. As the flow of nutrients into the Basin increases, this timescale generally becomes shorter so that if, say, a flushing event does introduce oxygen into the deep water these timescales indicate the approximate maximum time needed to reestablish anoxic conditions. The estimated times do not follow an entirely regular pattern. In particular, with sea level 60 m below present the model shows a very slow reduction rate in oxygen concentrations in the center of the west subbasin, presumably because there is little productivity over the center of that subbasin. This is because the nutrients entering the Basin have been consumed elsewhere (perhaps the east subbasin and shallower regions in general) before the waters carrying them reach the surface of the central west subbasin.

[29] It is perhaps notable that lamina preservation, as observed at ODP Site 1002, is less complete at the transition from the Bolling-Allerod (B/A) to the Younger Dryas and again from the Younger Dryas to the Preboreal. This suggests that flushing events occur more readily during climate transitions as the properties of the sea water outside the Basin changes more rapidly at these times. Indeed, analyses of sedimentary Molybdenum-Total Organic Carbon (Mo-TOC) values show that these parameters covary at the start of the Younger Dryas, inferring significant deep water renewal [*Algeo and Lyons*, 2006]. It is interesting to note that modern oceanographical data from the CARIACO time series station documents nonseasonal deep water intrusions into the Cariaco Basin in association with cyclo-

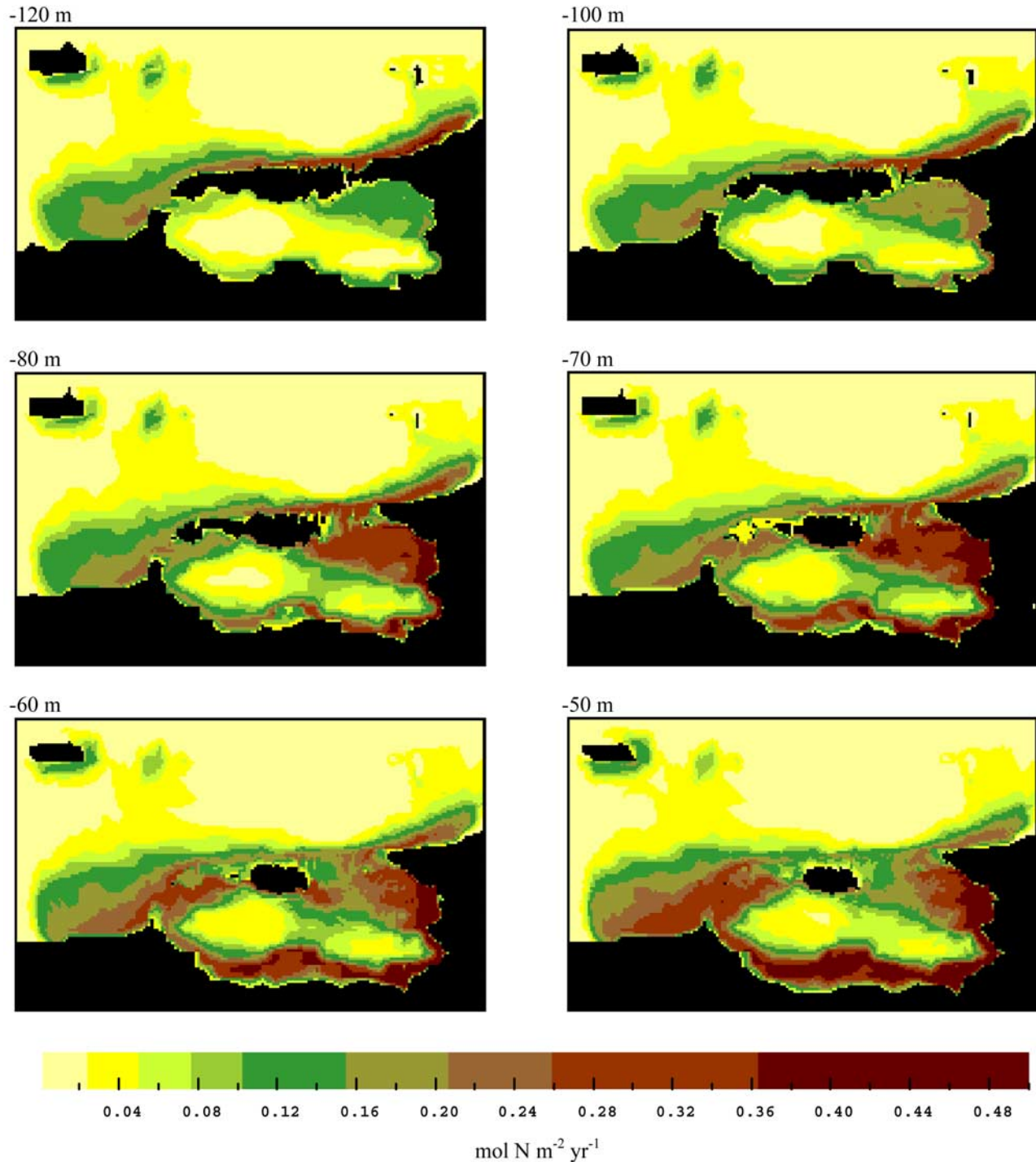


**Figure 9.** Annual marine sedimentation rate (in equivalent mole nutrient per square meter) for present-day climate forcing and various sea levels. The results are from year ten of each model run. As sea level rises, the maximum sedimentation occurs first in the shallow northeastern part of the Cariaco Basin and then over the Unare Platform in the south.

nic and anticyclonic eddies moving along the South American continental shelf [Astor *et al.*, 2003].

[30] The annual sediment deposition in year ten of each run is shown in Figure 9. For low sea level relatively little nutrient enters the Cariaco Basin and the weak sedimentation within the Basin is largely confined to the shallow region in the north east of the Basin and a narrow strip

around the southern coastline. As sea level rises the shallow northeast region still dominates the increasing sedimentation within the Basin but the southern boundary becomes gradually more important. By the time the sea level reaches 60 m below present, the Unare Platform is submerged and the largest sedimentation rates are found here and toward the southeast of the Basin. Overall, the main zone for

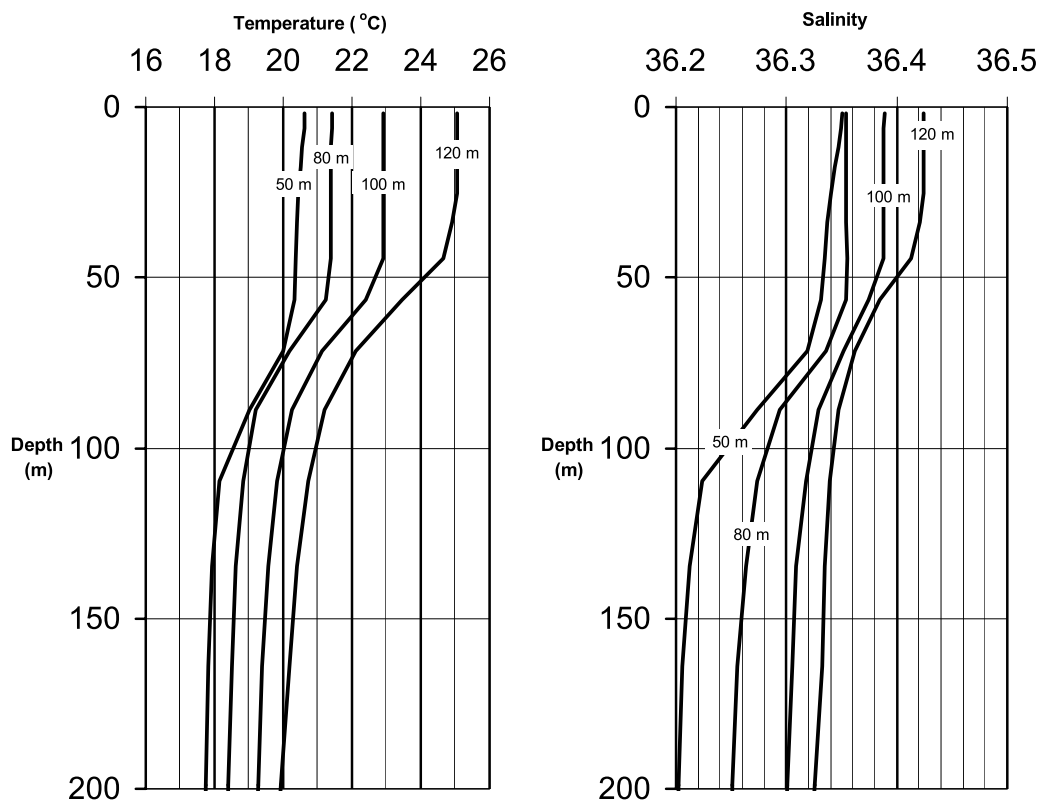


**Figure 10.** Model results for (a) temperature and (b) salinity profiles for the top 200 m of the water column in the center of the western subbasin of the Cariaco Basin at the end of 10-year runs. The results are for sea levels 50 m, 80 m, 100 m, and 120 m below present, as marked, corresponding approximately to 11 ka, 14 ka, 16 ka, and 21 ka B.P., respectively.

nutrient upwelling has moved from its initial position on the northern coasts of Tortuga and Margarita and the shallow strait between them to the northern coast of mainland South America. When the strait between Tortuga and Margarita was relatively shallow, the nutrient-rich deep waters were brought sufficiently close to the surface for biological production to occur. As this strait became deeper, the nutrient-rich waters, though brought up to a sufficiently shallow depth to flow over the sill into the Cariaco Basin, remain too deep for production until they are upwelled along the coasts in the southern and eastern parts of the Basin.

[31] The developing temperature and salinity profiles are shown in Figure 10. The lowering of the sill as sea level rises allows cooler, fresher water to enter the Cariaco Basin, and marginally deepens the overall depth of the surface mixed layer and the main circulation. However, the wind-driven circulation and mixing near the surface ensures that the circulation is not confined solely to the region above the sill depth, especially when this is very shallow. The temperature and salinity gradients are generally greater when the sea level is lower, since the slower overall circulation rate allows the surface waters to become hotter and saltier as they flow from the eastern side of the Cariaco Basin (where they are upwelled) westward to the main exit from the Basin. For example, the temperature difference over the top 100 m when the sea level was 120 m below present is approximately 4°C, whereas this reduces to 2.5°C when the sea level is 80 m below present.

#### 4.4. Case Study: ODP Site 1002

[32] Overall the nutrient supply, productivity and marine (or biogenic) sedimentation for the Cariaco Basin as a whole increases with increasing sea level (under the fixed surface forcing imposed here) but the distribution changes over time. We now consider the sedimentation at a particular location within the Cariaco Basin, namely the ODP Site 1002 which is on the northwestern part of the central saddle. Within each run, the amount of sedimentation at this location increases with time, appearing to tend toward a steady state value. The value of this steady state was estimated by fitting an exponential decay curve to the last four to six years of each run. For higher sea levels the system appears to take longer to approach the steady state, so the runs with sea levels of 70 m or less below present were extended by two years. The timescale for the decay curves was of the order of five to six years in all cases, giving an indication of the time for circulation and mixing within the Basin. The predicted biogenic sedimentation rate at the ODP site is shown in Figure 11. It increases as the sea level rises until the sea level is approximately 60 to 70 m below the present value (the predicted difference in sedimentation rate is smaller than the uncertainty in the curve fitting procedure). After that the sedimentation rate drops: This is the period when the main sedimentation zone moves south to the mainland coast. Thus, if the surface forcing remained constant, we would expect the sedimentation rate at the ODP site to rise from the LGM until 13 ka B.P. and

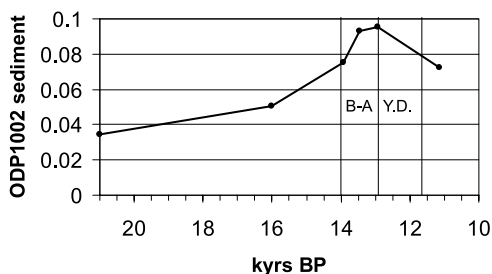


**Figure 11.** Predicted annual sedimentation rate (equivalent mole nutrient per square meter) at ODP Site 1002 from the model using present-day climate forcing (with linear interpolation between model results).

then fall. Deviations from this pattern indicate changes in climate. For example, the Younger Dryas (YD) was a period during which the climate differed significantly from the modeled conditions. It was a cool, dry period characterized by increased and/or more prolonged trade winds, so paleodata from this period should differ significantly from Figure 11. During the YD *Hughen et al.* [1996] record a substantial increase in light lamina thickness (a known proxy for biogenic productivity) from sediments in close proximity to ODP Site 1002. However, in Figure 11 the YD corresponds to a period when the model predicts declining sedimentation (if the surface forcing were the same as the present day). Thus the model clearly supports modulation of biogenic sedimentation by climate forcing during the YD, within the Cariaco Basin.

## 5. Comparison With Paleoceanographical Studies

### 5.1. Last Glacial Maximum

[33] The validity of the model results is supported by a number of similarities with published paleoceanographical data. The model suggests that at the LGM upwelling of deeper waters was active within the Cariaco Basin, and that the relatively low production was largely due to reduced levels of nutrient entering the Basin, as a result of the ingress of nutrient-depleted near-surface Caribbean waters (see discussion in the work of *Lin et al.* [1997] and *Haug et al.* [1998]). The model also shows that there would have been substantial upwelling and production to the north of the, then exposed, Tortuga Bank [*Peterson et al.*, 1991]. Furthermore, the model estimate of the temperature difference ( $4^{\circ}\text{C}$ – $4.5^{\circ}\text{C}$ ) between the surface waters of the Cariaco Basin and those at a depth of 100 m compares favorably with  $\delta^{18}\text{O}$  foraminiferal faunal data [*Lin et al.*, 1997]. This thermal gradient is a result of two hydrographic features. The model draws into the Basin relatively cool waters from below the sill depth during the LGM lowstand ( $-120$  m sea level). Earlier studies suggest that during the LGM, the temperature in the upper water column did not fall below that at the sill depth [*Lin et al.*, 1997]. However, the model infers that Ekman-induced upwelling of nutrient-rich waters from depths greater than 25 m is active outside of the Basin during the LGM, and that the inward flow of water across the sill incorporates some of this cool “upwelled” water (Figure 7c). In addition, water upwelled in the east of the Cariaco Basin is warmed by insolation as it flows northwestward, further enhancing the vertical temper-

ature gradient. The net result of these hydrographic features is a LGM SST of approximately  $25^{\circ}\text{C}$  in the western subbasin (Figure 10), as compared with  $24^{\circ}\text{C}$  in the eastern subbasin. (Note this prediction does not include any correction for a cooler, glacial Caribbean Sea.)

[34] Previous geochemical, micropalaeontological and sedimentological studies show that during the LGM the water column within the Cariaco Basin was at least moderately well ventilated [*Peterson et al.*, 1991; *Dean et al.*, 1999]. However, model runs for a sea level below present of  $-120$  m using surface forcing associated with a southward displaced ITCZ, indicate that anoxia will still develop within the Cariaco Basin, over a timescale of several hundred years (Table 1). By inference, during glacial times, surface production and the associated oxygen demand created by oxidizing sinking organic detritus, would still have been too high to maintain oxic conditions within the deeper waters of the Cariaco Basin. To maintain a steady state the model requires an additional source of oxygen. From studies of the Basin, it is known that the most likely source of oxygen is from the periodic downwelling of oxygen-enriched, relatively saline waters (though diffusion alone will maintain a small supply of oxygen to the deep water). However, the model does not increase surface water salinities significantly above those experienced in the modern basin. Despite this, there is modern and paleoceanographical evidence to suggest that downwelling of relatively dense, oxygenated waters has and does occur [*Holmén and Rooth*, 1990; *Herbert and Schuffert*, 2000; *Astor et al.*, 2003]. Furthermore, *Peterson et al.* [2000a] have suggested that flushing events involving saline surface waters would have been enhanced during the LGM and earlier glacials, given the restricted Basin circulation and increased aridity associated with a southward shift in the ITCZ and its accompanying rain belt.

### 5.2. Last Deglacial Transition

[35] Using present-day climate parameters, the SST of the western subbasin (Figure 10) shows a gradual cooling trend from a maximum sea level low stand of  $-120$  m through to  $-50$  m. Two linked processes can account for this. During the last deglacial transition there is an increased rate of flow of water into the Basin through both the NW and N straits. As previously suggested by *Herbert and Schuffert* [2000] and described by the current model, during periods of rising sea level cooler deeper waters are drawn across the deeper sill connections. After upwelling of these waters in the east of the Cariaco Basin, this increased volume of now surface water is not warmed as significantly by insolation, during its movement from E-W across the Cariaco Basin, as during the LGM. The net effect of this is to lower the modeled SST in the Cariaco Basin, as sea level rises. During the Younger Dryas, the stronger trade winds [*Lin et al.*, 1997; *Haug et al.*, 1998] would have further enhanced the processes and effects cooling the SST described above. Cloud cover is not included in the model, but might be expected to reduce insolation heating during the warmer/wetter B/A as compared with the cooler/drier Younger Dryas. However, the model is using a modern climatology, with fixed, present day, temperature values for the Caribbean waters. Paleo-SST records indicate an oscillating, but warming trend in Cariaco SST during the last glacial transition [*Lea et al.*,

2003], which suggests the incoming waters must be warmer to counteract the cooling trend that the model shows would otherwise occur as sea level rises.

[36] The model data showing the time required for the development of anoxia during the last deglacial transition (Table 1) assume a fully oxygenated state in the deep waters of the Cariaco Basin. The model does not account for the likelihood of a partially oxygenated basin [Peterson *et al.*, 1991; Dean *et al.*, 1999], or increases (or decreases) in the input of riverine nutrients, which for example are likely to have abruptly risen at the onset of the wet B/A [Hughen *et al.*, 2004]. It is likely the effects of these factors reduced the onset time for anoxic conditions at the start of the B/A, sufficiently to complete an already well-advanced transition from oxic to anoxic deepwater. When the modeled levels of anoxia are put into the context of a partially oxygenated Basin, they favorably describe the conditions estimated from paleodata. The modeled rate of oxygen depletion in the early part of the B/A, i.e.,  $-80$  m below current sea level datum, modifies the basin waters from dysoxic to suboxic/anoxic (1 ml/L to 0 ml/L) over a period of about 30 years. This is of similar order of magnitude to the estimate of the onset of anoxia, deduced from sedimentary and micro-paleontological records [Peterson *et al.*, 1991]. In the Cariaco Basin concentrations of Mo, which are used as a proxy for anoxic conditions, show an abrupt rise a few hundred years prior to the onset of laminated sediments and anoxic bottom water conditions [Dean *et al.*, 1999]. Again a comparable timescale to develop anoxia within the deeper waters of the Cariaco Basin is estimated by the model (see Table 1).

### 5.3. Conclusions and Future Work

[37] The numerical model allows us to see how the pattern of sedimentation and hydrography in the Cariaco Basin changes in response to the rise in sea level. One should exercise some caution in using the precise quantitative results, since there is not sufficient data to do detailed calibrations. However, the overall patterns, trends and relative scalings should be sound, and a comparison with paleodata provides a useful validation of the model results. Within the Cariaco Basin changes in forcing are more likely to affect the strength of circulation and the amount of primary production and sedimentation, while the estuarine-like character (flow entering the Basin at depth and leaving the Basin at the surface) remains essentially unaltered.

[38] An important observation to be made from the numerical model is the care that is needed in interpreting observations from a particular core site. The behavior at individual sites will not always mirror the regional response and the observations are also modified by changes in the physical topography, for example from sea level rise, and whether the location is in the western or eastern subbasin, as well as by changes in climate or other conditions. The model could, for example, be used to address the differences in observed sedimentation rates at core sites V12-104 and V12-99 [Peterson *et al.*, 1991], though in the present runs of the model the difference in sedimentation between these two sites is strongly affected by the oxygenated deep waters, in that more detritus is remineralized as it falls to the deeper V12-99 site (depth  $-1005$  m) than the shallower

V12-104 site ( $-466$  m). The model also highlights the influence of insolation in heating surface waters in the basin, as well as the source depth of water inflowing across the sills.

[39] In the numerical model only the marine (biogenic) sediment component resulting from nutrient imported into the Cariaco Basin from the open ocean has been modeled, whereas the laminated sediments from the Cariaco Basin have terrigenous components and other nutrient sources. The terrigenous components are linked to local rainfall, which in turn is strongly related to the location and migration of the ITCZ. In the future, the aim will be to use detailed numerical modeling (varying climate and topography) to give more precise interpretations of the sediment record and thus to be able to reconstruct even more detailed tropical paleoclimate with some confidence. This type of model could also be used to address such questions as to why laminations occur in some periods of similar sea level and not in others (e.g., laminations are observed in Marine Isotope Stage (MIS) 3, but are largely absent from MIS 5, except for a short sequence in MIS 5e).

[40] **Acknowledgments.** We would like to thank the OCCAM team and also George Nurser from the National Oceanography Centre, Southampton (UK) for help and advice on the numerical modeling. We would also like to thank the referees for their detailed and helpful comments and Larry Peterson for commenting on an earlier version of the manuscript.

### References

- Algeo, T. J., and W. Lyons (2006), Mo-total organic carbon covariation in modern anoxic marine environments: Implications for analysis of paleoredox and paleohydrographic conditions, *Paleoceanography*, *21*, PA1016, doi:10.1029/2004PA001112.
- Anderson, L. A., and J. L. Sarmiento (1994), Redfield ratios of remineralization determined by nutrient data-analysis, *Global Biogeochem. Cycles*, *8*(1), 65–80.
- Astor, Y., F. Muller-Karger, and M. Scranton (2003), Seasonal and inter-annual variation in the hydrography of the Cariaco Basin: Implications for basin ventilation, *Cont. Shelf Res.*, *23*(1), 125–144.
- Bryden, H. L., and T. H. Kinder (1991), Steady 2-layer exchange through the Strait of Gibraltar, *Deep Sea Res. Part I*, *38* (suppl. 1), S445–S463.
- Chiang, J. C. H., M. Biasutti, and D. S. Battisti (2003), Sensitivity of the Atlantic Intertropical Convergence Zone to Last Glacial Maximum boundary conditions, *Paleoceanography*, *18*(4), 1094, doi:10.1029/2003PA000916.
- Dalziel, S. B. (1992), Maximal exchange in channels with nonrectangular cross-sections, *J. Phys. Oceanogr.*, *22*(10), 1188–1206.
- Dean, W. E., D. Z. Piper, and L. C. Peterson (1999), Molybdenum accumulation in Cariaco Basin sediment over the past 24 k.y.: A record of water-column anoxia and climate, *Geology*, *27*(6), 507–510.
- Fairbanks, R. G. (1989), A 17,000-year glacio-eustatic sea level record: Influence of glacial melting rates on the Younger-Dryas event and deep-ocean circulation, *Nature*, *342*, 637–642.
- Haug, G. H., T. F. Pedersen, D. M. Sigman, S. E. Calvert, B. Nielsen, and L. C. Peterson (1998), Glacial/Interglacial variations in production and nitrogen fixation in the Cariaco Basin during the last 580 kyr, *Paleoceanography*, *13*, 427–432.
- Herbert, T. D., and J. D. Schuffert (2000), Alkenone unsaturation estimates of sea-surface temperatures at Site 1002 over a full glacial cycle, in *Proceedings of the Ocean Drilling Program, Scientific Results*, vol. 165, edited by R. M. Leckie *et al.*, pp. 239–247, College Station, Tex.
- Holmén, K. J., and C. G. H. Rooth (1990), Ventilation of the Cariaco Trench, a case of multiple source competition?, *Deep Sea Res. Part I*, *37*(2), 203–225.
- Hughen, K. A., J. T. Overpeck, L. C. Peterson, and S. Trumbore (1996), Rapid climate changes in the tropical Atlantic region during the last deglaciation, *Nature*, *380*, 51–54.
- Hughen, K. A., T. I. Eglinton, L. Xu, and M. Makou (2004), Abrupt tropical vegetation response to rapid climate changes, *Science*, *304*(5679), 1955–1959.
- Josey, S. A., E. C. Kent, and P. K. Taylor (1999), New insights into the ocean heat budget closure problem from analysis of the SOC air-sea flux climatology, *J. Clim.*, *12*(9), 2856–2880.

- Lane-Serff, G. F., E. J. Rohling, H. L. Bryden, and H. Charnock (1997), Postglacial connection of the Black Sea to the Mediterranean and its relation to the timing of sapropel formation, *Paleoceanography*, *12*(2), 169–174.
- Lea, D. W., D. K. Pak, L. C. Peterson, and K. A. Hughen (2003), Synchronicity of tropical and high-latitude Atlantic temperatures over the last glacial termination, *Science*, *301*(5638), 1361–1364.
- Lin, H.-L., L. C. Peterson, J. T. Overpeck, S. E. Trumbore, and D. W. Murray (1997), Late Quaternary climate change from  $\delta^{18}\text{O}$  records of multiple species of planktonic foraminifera: High resolution records from the anoxic Cariaco Basin, Venezuela, *Paleoceanography*, *12*, 415–427.
- NOAA (1988), *Data Announcement 88-MGG-02, Digital Relief of the Surface of the Earth*, Natl. Geophys. Data Cent., Boulder, Colo.
- Pacanowski, R. C., K. Dixon, and A. Rosati (1990), *The GFDL Modular Ocean Model 1.0.*, Geophys. Fluid Dyn. Lab./NOAA, Princeton Univ., Princeton, N. J.
- Peterson, L. C., and G. H. Haug (2006), Variability in the mean latitude of the Atlantic Intertropical Convergence Zone as recorded by riverine input of sediments to the Cariaco Basin (Venezuela), *Palaeogeogr. Palaeoclimatol. Palaeoecol.*, *234*(1–2), 97–113.
- Peterson, L. C., J. T. Overpeck, N. G. Kipp, and J. Imbrie (1991), A high-resolution Late Quaternary upwelling record from the anoxic Cariaco Basin, Venezuela, *Paleoceanography*, *6*, 99–119.
- Peterson, L. C., G. H. Haug, R. W. Murray, K. M. Yarincik, J. W. King, T. J. Bralower, K. Kameo, and R. B. Pearce (2000a), Late Quaternary stratigraphy and sedimentation at ODP Site 1002, Cariaco Basin (Venezuela), in *Proceedings of the Ocean Drilling Program, Scientific Results*, vol. 165, edited by R. M. Leckie et al., pp. 85–99, College Station, Tex.
- Peterson, L. C., G. H. Haug, K. A. Hughen, and U. Röhl (2000b), Rapid changes in the hydrologic cycle of the tropical Atlantic during the last glacial, *Science*, *290*(5498), 1947–1951.
- Richards, F. A. (1975), The Cariaco Basin (Trench), *Annu. Rev. Oceanogr. Mar. Biol.*, *13*, 11–67.
- Richards, F. A., and R. F. Vaccaro (1956), The Cariaco Trench, an anaerobic basin in the Caribbean Sea, *Deep Sea Res.*, *3*(3), 214–228.
- Smith, W. H. F., and D. T. Sandwell (1994), Bathymetric prediction from dense satellite altimetry and sparse shipboard bathymetry, *J. Geophys. Res.*, *99*(B11), 21,803–21,824.
- Smith, W. H. F., and D. T. Sandwell (1997), Global sea floor topography from satellite altimetry and ship depth soundings, *Science*, *277*(5334), 1956–1962.
- Stratford, K., R. G. Williams, and P. G. Myers (2000), Impact of the circulation on sapropel formation in the eastern Mediterranean, *Global Biogeochem. Cycles*, *14*(2), 683–695.
- Walsh, J. J., et al. (1999), Simulation of carbon-nitrogen cycling during spring upwelling in the Cariaco Basin, *J. Geophys. Res.*, *104*(C4), 7807–7825.
- Webb, D. J. (1993), An ocean model code for array processor computers, *Comput. Geosci.*, *22*(5), 569–578.
- Webb, D. J. (1998), Improved advection schemes for ocean models, *J. Atmos. Ocean. Technol.*, *15*, 1171–1187.

---

G. F. Lane-Serff, School of Mechanical, Aerospace and Civil Engineering, University of Manchester, P.O. Box 88, Sackville Street, Manchester M60 1QD, UK. (gregory.f.lane-serff@manchester.ac.uk)

R. B. Pearce, School of Ocean and Earth Science, University of Southampton, National Oceanography Centre Southampton, European Way, Southampton SO14 3ZH, UK. (r.pearce@noc.soton.ac.uk)